Optical Materials 66 (2017) 247–252

Contents lists available at ScienceDirect

Optical Materials

journal homepage: www.elsevier.com/locate/optmat

Azopolymer film as an actuator for organizing multiwall carbon nanotubes

Maria Gabriela Capeluto [a, *], Raquel Fernández Salvador [c], Aranxa Eceiza [c], Silvia Goyanes [b], Silvia Adriana Ledesma [a]

[a] Laboratorio de Procesado de Imágenes (LPI), Departamento de Física, Facultad de Ciencias Exactas y Naturales, Universidad de Buenos Aires and IFIBA, CONICET, Cuidad Universitaria, Buenos Aires, 1428, Argentina
[b] Laboratorio de Polímeros y Materiales Compuestos (LPM&C), Departamento de Física, Facultad de Ciencias Exactas y Naturales, Universidad de Buenos Aires and IFIBA, CONICET, Cuidad Universitaria, Buenos Aires, 1428, Argentina
[c] Grupo "Materiales + Tecnologías", Departamento de Ingeniería Química y del Medio Ambiente, Escuela de Ingeniería de Gipuzkoa, Universidad del País Vasco, Pza Europa 1, 20018, Donostia-San Sebastián, Spain

ARTICLE INFO

Article history:
Received 31 October 2016
Received in revised form
24 December 2016
Accepted 25 January 2017

Keywords:
Azopolymer
Surface relief gratings
Multiwall carbon nanotubes
Actuator

ABSTRACT

In this work we show the feasibility of using an azopolymer as an actuator to induce nano- and microscale movements controlled with light from the far field. We study azopolymers and their interaction with multi-walled carbon nanotubes (MWCNTs) by inducing surface relief gratings (SRG) through optical illumination. Upon different optical treatments, the MWCNTs are organized in the troughs or the crests of a surface relief grating. Large scale organization of MWCNTs has potential in applications such as transparent electronics.

© 2017 Elsevier B.V. All rights reserved.

1. Introduction

Light activated optical actuators are probably the least developed force-generating structures, however they offer several interesting features based on the capability to transform the properties of light (radiation pressure, intensity, wavelength, phase) in displacements and forces. A distinctive characteristic is that they allow the remote optical to mechanical energy conversion and its coupling into small systems. Consequently, they enable the electro-mechanical decoupling since they are activated by light instead of currents or voltages, eliminating the need of circuitry [1].

Among other materials such as single-DNA nanomotors [2], molecular photo-switches [3] or liquid crystal molecules [4], azopolymers are one of the most promising photo-responsive materials since they exhibit large macroscopic directional motion and changes in shape when exposed to light. In fact, the works of Ikeda et al. about photo induced motion in liquid crystalline azopolymers, have had remarkable impact in the scientific community [5–7]. An azopolymer is a physical mixture or a chemical functionalization of a polymer and an azobenzene dye. Under exposure to light with a particular wavelength, azobenzene molecules undergo a reversible conformational E-Z transition (between the cis and trans states) [8]. When the irradiation light is polarized, photo-selective isomerization conducts to the orientation of the transition dipole moment of the molecules perpendicular to light polarization [9]. The same effect, observed as optical induced anisotropy (birefringence and dichroism) when illuminating a material in bulk, has proven useful for applications in reversible optical memory storage [10–12].

The nanoscale photoisomerization reaction is also responsible for the large scale molecular motion of the polymer when the azo dye is chemically bonded to the polymer chain. In this case, the collective motion of the azopolymer molecules is observed as a macroscopic mass transport driven by light. Despite the fact that the phenomenon of mass transport is still under debate, the large deformation of the material that is observed when the azopolymer is illuminated with light polarization or intensity gradients (even below Tg), opens up the possibility of creating a wide variety of applications. Besides the classical applications like lithography

* Corresponding author.
E-mail address: maga@df.uba.ar (M.G. Capeluto).

http://dx.doi.org/10.1016/j.optmat.2017.01.047
0925-3467/© 2017 Elsevier B.V. All rights reserved.

[13,14], optically induced mass transport in azopolymers is suited for new innovative applications like cell culture [15,16], plasmonic sensors [17] or lasers [18,19].

Few works can be found using azo compounds as light driven technologies to manipulate nano and microscale objects. The photo-responsive properties of the material have been used to organize polystyrene nano particles [8,20], to selective pattern self-organized colloids through photo-immobilization [21] or through azopolymer nanosphere deformation [22,23]. However, azopolymers haven't been used to organize carbon nanotubes (CNT) until now. CNT have diameters of tens of nanometers but their length is in the microscale, which makes them excellent candidates to connect the nano and micro world. In fact, it is well known that carbon nanotubes have exceptional strength and stiffness as well as extraordinary thermal and electrical properties. Large scale organization of CNT is interesting because of its potential use in applications such as transparent electronics. Achieving parallel aligned and interconnected conducting CNT, could help to produce electrical contacts with lateral dimension in the nanoscale while connecting components at meso or microscale distances.

In this work we report large area organization of multiwall carbon nanotubes (MWCNTs) using azopolymer films. This is accomplished by the inscription of surface relief gratings before and after the deposition of a solution containing the dispersed MWCNTs. This kind of organization could have potential applications where long linear contacts or an array of parallel aligned contacts are required.

2. Experimental

2.1. Materials

Reagent grade methanol, ethylene glycol and tetrahydrofuran (THF) from Biopack (Argentina) were used in our experiment to develop the materials. Dispersed Orange 3 (DO3) dye and poly[1-[4-(3-carboxy-4-hydroxyphenylazo) benzenesulfonamido]-1,2-ethanediyl, sodium salt] (PAZO) were acquired from Sigma-Aldrich and MWCNTs from Nanocyl (NC3100). The mean length of the MWCNTs is about 1.5 μm and their diameter is around 20 nm [24].

We fabricated an azo compound based on a commercial azopolymer (PAZO), a plasticizer (ethylene glycol) and a solvent (methanol). DO3 was used as a dispersive agent of MWCNT. As it was demonstrated by our group in previous works [24], DO3 is an excellent disperser of MWCNT when using THF. Since DO3 is used in a solution, its molecules are found as a monomer or dimer. In addition, the DO3/PAZO ratio is less than 0.03. As a consequence, DO3 has a negligible influence in the photo induced properties of the material, being PAZO the most significant component of the azo compound.

2.2. Film preparation and characterization

Azopolymer compound was fabricated by dissolving 100 mg of PAZO in 1 mL methanol and 0.3 mL ethylene glycol using an ultrasonic bath for 30 min. The resulting homogeneous solution was deposited as thin layers on a clean coverslip by spin coating at a speed of 3600 rpm. We dropped a 100 μL volume of the solution, and let it spin for 1 min, repeating the process 3 times. The methanol in the samples was evaporated in a furnace, using a stepped rising temperature protocol that allows for the production of homogeneous thin films without bubbles. The temperature sequence used was 12 h at 50 °C, 2 h at 60 °C and 2 h at 80 °C. The resulting film thickness of about 0.9 μm was measured from cryogenic fractured surface of the samples using an SEM. Fig. 1 shows

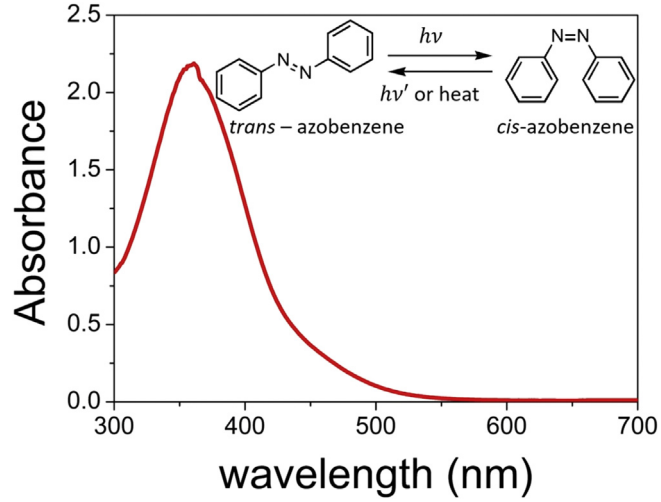

Fig. 1. UV–vis spectra of a sample prepared as a thin film consisting of a strong absorption band peaking at360 nm and 100 nm FWHM. Inset: schematic of the E-Z photo-isomerization (*cis-trans*) of azo dye molecule. The molecule switches between the *cis* and *trans* states by absorbing photons. Thermal relaxation is also possible from *cis* to *trans* state.

the absorption UV–visible spectrum of a typical sample that is composed of a wide band peak centered in 360 nm and FWHM of 100 nm. In order to isomerize the azopolymer, we used photons at 473 nm wavelength from a diode laser with 50 mW power. This wavelength falls into the absorption band of the samples.

Samples were characterized by Atomic Force Microscopy (AFM) and Scanning Electron Microscopy (SEM). For the second technique we sputtered a thin layer of platinum (10 nm thick) to avoid charging of the polymer film while electrons hit the sample.

2.3. MWCNTs solutions

In order to prevent MWCNT agglomeration, we dispersed them in THF by the addition of a small amount of DO3. As it was demonstrated by Costanzo et al. [24], the π-π stacking interactions between MWCNTs and an azobenzene derivative (DO3) allows debundling of MWCNTs in a dispersed solution persistent for days. The main advantage of using THF is that PAZO is not soluble in it, making feasible the deposition of MWCNTs on the azopolymer films. Before preparing the dispersed solution, MWCNTs and DO3 were dried in a vacuum furnace at 120 °C during 2 h to remove adsorbed water and they were left in vacuum at room temperature until used. In order to study the ordering capability of the polymer to organize either well dispersed MWCNTs or its agglomerates, we produced solutions with different concentrations of MWCNTs. We kept constant the amount of THF (3.5 mL) and DO3 (10 mg), being the last one the only photo-isomerizable component in the mixture. Herein we used2.4 mg of MWCNTs for the lower concentration and 4.8 mg of MWCNTs for the higher one.

The MWCNTs solution was deposited on the sample by spin coating, either before or after illuminating the sample. We spin coated drops with a volume of 100 μL, during 1 min at a speed of 3600 rpm.

2.4. SRG recording

The Lloyd's mirror interferometer scheme used in this experiment was previously employed to study photo-induced properties in azopolymer films [10,25] in our group. In this wavefront division interferometer, part of a beam impinged on the mirror at grazing

incidence angle (θ) and was reflected to interfere with the remaining undeflected portion of the beam. Beam interference gave rise to a sinusoidal intensity pattern of period $d = \lambda/2\sin(\theta)$, defined by the angle θ and the wavelength of the light λ.

The complete schematic of the experimental setup used in this experiment is shown in Fig. 2 (a). A 473 nm laser was filtered and magnified using a spatial filter composed by a 10× objective Melles Griot (O), a lens (L) and a50 μm diameter pinhole (PH). The resulting beam width was 2 mm FWHM. The transmission axis of the polarizer (P) was set in the x direction, so the interference beams were p-polarized. A half wave plate (HWP) was used to optimize the intensity on the sample. The Lloyd mirror (M) was set at an angle of 5° respect to the incident beam direction. The sample (F) was mounted perpendicular to the mirror. The average power density on the sample was 0.2 W/cm^2 approximately.

In this experiment a p-polarized laser impinged on the mirror at an angle of about 5° obtaining a fringe period of about 2.7 μm. When the laser is p-polarized laser and the incidence angle is smaller than π/4, a large modulation of the polarization is obtained across the fringes aside from the intensity gradient. In this case the intensity (I) distribution can be computed using simple geometrical optics:

$$I = I_o\left(1+\rho^2\right)\left[1+\frac{2\rho}{1+\rho^2}\cos(2\theta)\cos(2k_o\,\sin(\theta)u)\right], \qquad (1)$$

where I_o is the incident intensity, ρ is the reflectivity of the mirror for photons of wavelength λ at the angle of incidence θ, $k_o = 2\pi/\lambda$, and u the coordinate along the sample. A schematic of the distribution of intensities and polarization can be observed in Fig. 2(b).

3. Results and discussion

Azopolymer SRG was imprinted on a large area of the film that corresponds to the portion of the sample illuminated by the beam. Fig. 3 (a) shows a picture of the diffraction on SRG that was recorded during 13 h, on an area of about (~6 mm^2). The filtered and expanded laser used for illumination has a Gaussian intensity distribution profile. Since Lloyd mirror interferometer produces the superposition of two halves of the beam, the irradiance on the sample, that is the interference pattern, is modulated by a squared Gaussian distribution with a maximum near the center of the flat edge where the beam is folded, as is indicated in Fig. 3(a). As a result, it is expected that the modulation depth of the recorded SRG decreases radially from the location of the maxima. Fig. 3(b) and (c) show an AFM image and an image profile of the SRG measured in the area where the intensity has a maximum value, i.e. where the modulation is higher. The modulation depth measured from the AFM profile is about800 nm (1.69 λ).

In order to study MWCNTs organization in azopolymer films, two fabrication processes were used: the deposition of MWCNTs before or after illumination. In the first case, we show the results for the lower concentration of MWCNTs, where they are completely dispersed or in small agglomerates. In second case, we show the results for the higher concentration, where the MWCNTs are part of larger agglomerates.

The results for lower concentration are shown in Figs. 4–6. Fig. 4 (a) shows a SEM image of a large area (~31μmX23 μm) of a sample where we spin coated 3 drops of the MWCNTs solution on a recorded SRG. The SRG crests in the image are clean of MWCNTs, instead they are located in the troughs. This organization could be attributed to the fact that there are different mechanical forces acting at different locations. MWCNTs that initially fall in the crest, could be flung out of the sample or fall into a trough, because of the action of the inertial forces (that are parallel to the substrate) during the spinning of the spin coater. On the other hand, a MWCNT that falls in the trough will probably stay in there. This could be due to the existence of an additional contact force between the MWCNTs and the walls of the SRG, parallel to the inertial forces but in opposite direction. In order to get an insight about the film evolution and the initial smoothness of the film before irradiation, we show in the Supplementary Materials, SEM images of the different stages on fabrication. It could also be possible another interaction force related to the π-π stacking between the phenyl rings in the azocompound DO3 that is linked to the MWCNTs and the phenyl rings in the chromophore in PAZO. Fig. 4 (b) shows a magnified area of the sample where MWCNTs are located, with some of them aligned along the trough of the SRG. This indicates that this method could be a route to produce long MWCNTs contacts or an array of MWCNTs contacts, taking advantage of the fact that MWCNTs can conduct electricity.

The results change significantly when the SRG is recorded after the deposition of the MWCNTs. Fig. 5(a) shows an SEM image of a sample in which we spin coated 3 drops of MWCNTs solution and then it was irradiated with the interference pattern for 13 h. Very few MWCNTs are visible in the surface suggesting they were covered by the material while the relief grating was recorded. Fig. 5(b) shows a magnified view of a bundle of MWCNT sunk partially in the SRG. Despite the fact that some part of the MWCNT bundle is outside of the material, it is clearly seen that the MWCNT are coated by the polymer since they have greater thickness than the MWCNT measured on Fig. 4(b). However, in general, there are some irregularities on the surface of the SRG crests, indicating that there are more MWCNT deep into the material. It is possible that these MWCNTs were moved to the crest, while the mass was transported from higher to lower intensity illuminated areas. Moreover, regarding the high volume of mass transported, the MWCNT ended up completely covered by the azopolymer. When the concentration of MWCNTs increases the surface is more irregular as it will be shown later.

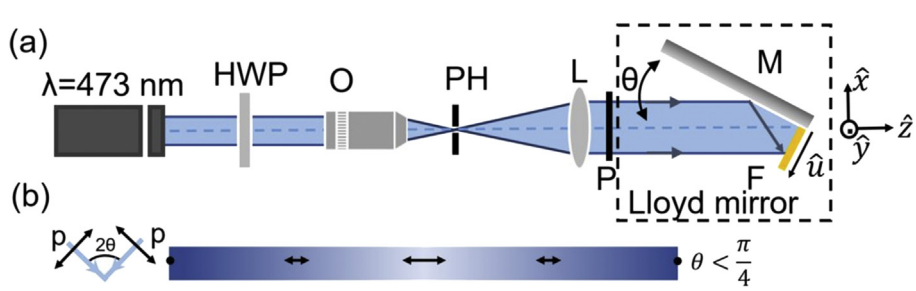

Fig. 2. (a) Experimental setup used for recording the SRG. A spatially filtered and expanded 473 nm laser beam impinges on a Lloyd mirror interferometer. The sample (F) is mounted normal to the mirror. HWP: half waveplate, O: objective, PH: pinhole, L: lens, P: polarizer, M: mirror. (b) Schematic of the intensity (pseudo color blue) and polarization (arrows) distribution for p-p interfering beams, along the coordinate $\hat{u}$ measured on the sample, for a small angle of incidence $\theta < \frac{\pi}{4}$. (For interpretation of the references to colour in this figure legend, the reader is referred to the web version of this article.)

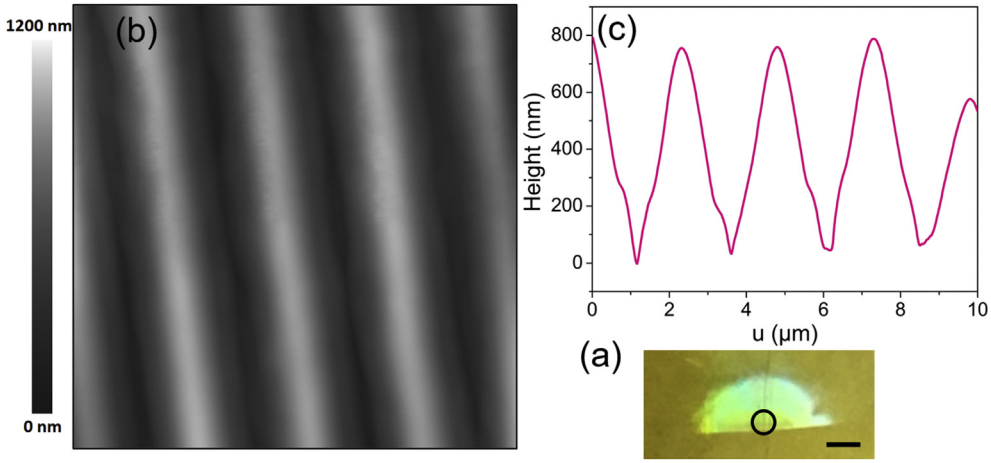

Fig. 3. (a) Picture of a large area printed SRG, the square indicates the imprinted area of larger modulation depth. Scale bar equals 1 mm. (b) AFM image of a 10 μm × 10 μm area, measured on the higher modulation depth expected location. (c) Profile taken on a line perpendicular to the grating grooves on the AFM image.

Fig. 6 shows that higher concentrations of MWCNTs have the same behavior in terms of organization, i.e. when nanotubes were deposited before or after the recording of the SRG, they locate in the crests or troughs of the SRG respectively. In the case of higher concentrations, we found the MWCNTs being part of an interconnected spatially extended network that occupied a large area of

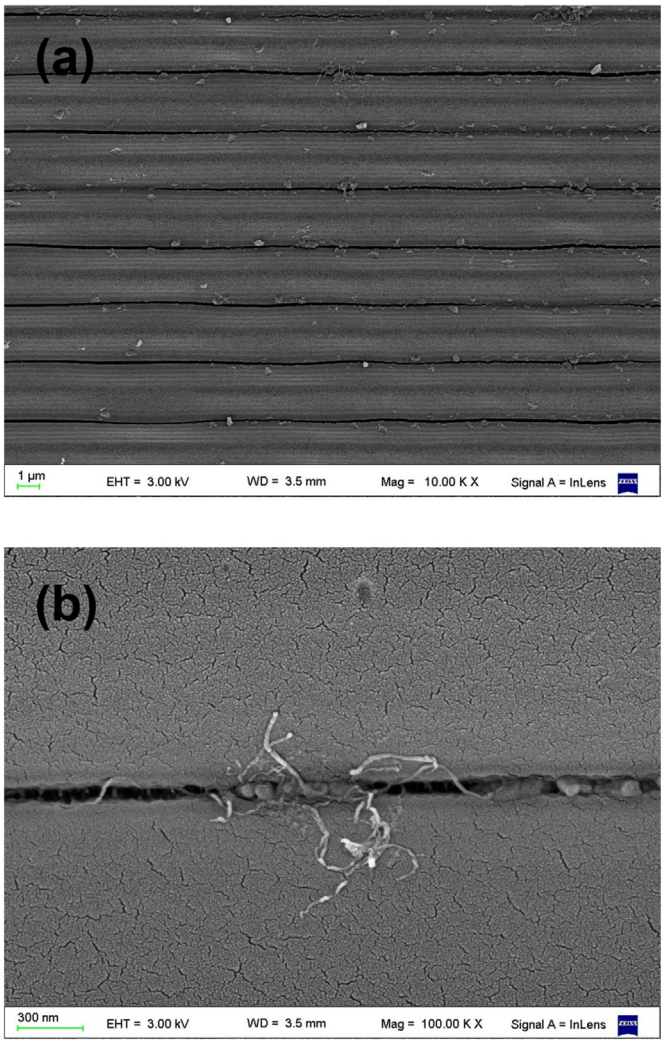

Fig. 4. (a) SEM image of a 13 h recorded SRG. MWCNTs were deposited after recording the grating. (b) Magnified area where CNTs are observed in the troughs of the SRG.

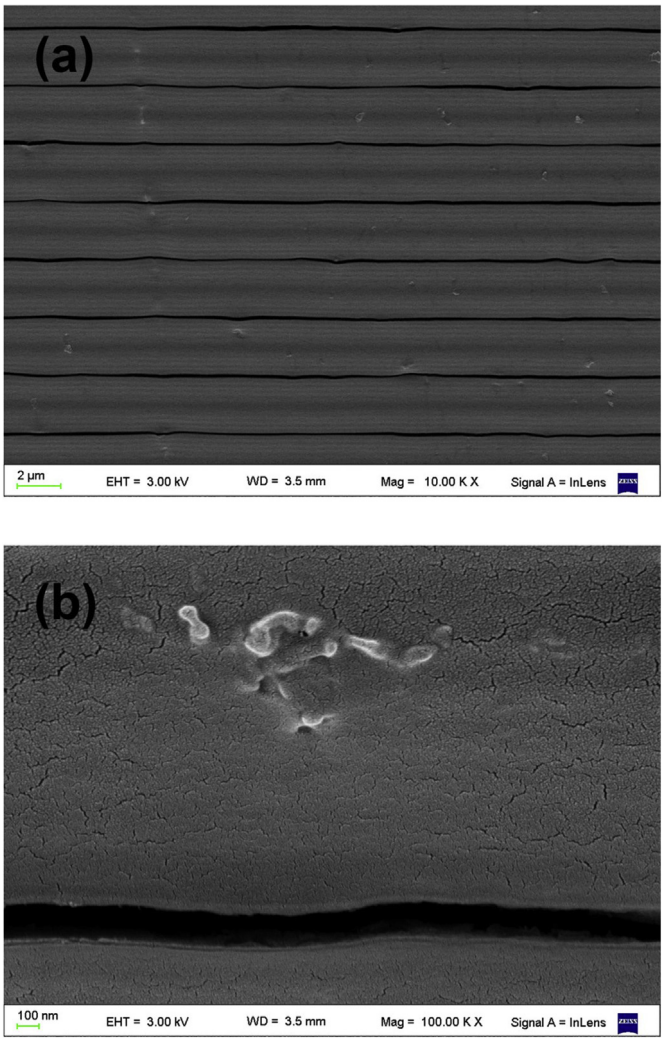

Fig. 5. (a) SEM image of a 13 h recorded SRG. MWCNTs were deposited before recording the grating. (b) Magnified area where CNTs are partially sink in the SRG crest.

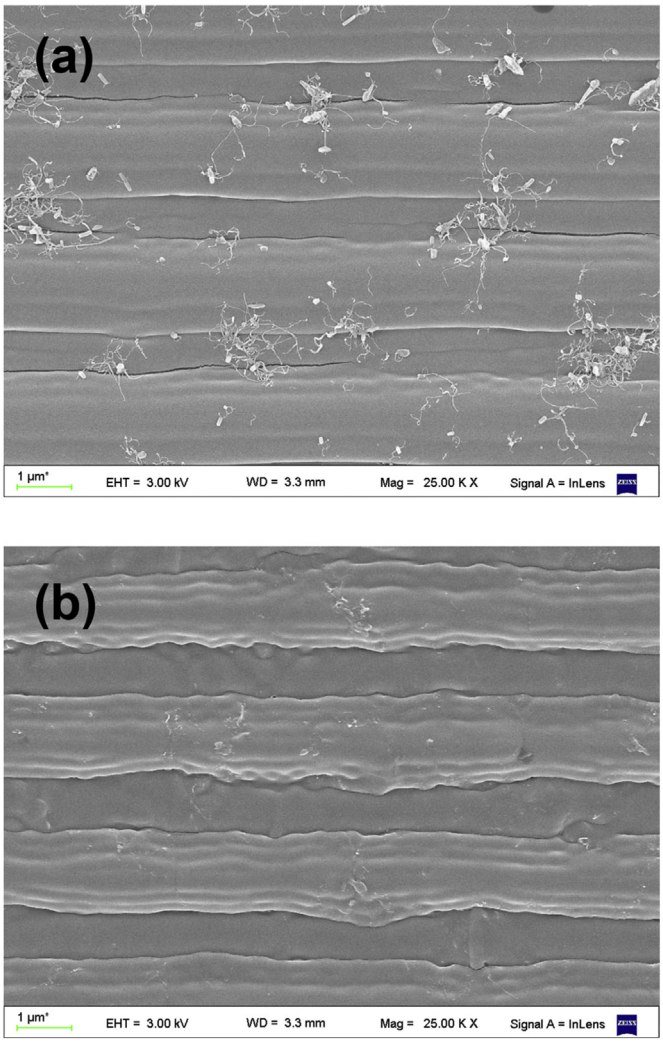

Fig. 6. SEM images of two samples fabricated from a solution with higher concentration of MWCNTs that were irradiated with an interference pattern before (a) and after (b) the deposition of the solution.

about the same order of the SRG period, instead of a small agglomerate of MWCNTs or single nanotubes. This is probably due to the lower availability of DO3 for dispersing higher amount of MWCNTs. As it was expected from the results for low concentration (Figs. 4 and 5), when MWCNTs networks were deposited after irradiation, they were mainly distributed in the troughs of the SRG. On the other hand, when the MWCNTs networks were deposited before irradiation they were mainly distributed in the crests. Fig. 6 shows SEM images exhibiting the same behavior discussed previously. However, a huge deformation of the polymer matrix is observed when MWCNTs networks are deposited before the irradiation of the sample. This deformation could arise from the differences in the dragging forces required for the azopolymer to move the different objects. Higher dragging forces are expected when trying to move the MWCNTs network due to the higher surface to volume aspect ratio in comparison with the more compact configurations (small agglomerates or single objects). This explains why in the first case, the SRG is more regular. In spite of pristine organized matter, there might be a limit in the surface to volume ratio of the nanostructure that allows the azopolymer to move the nanostructures without changing the morphology of the SRG. This kind of deformation was previously observed by Snell et al. [8] using silica nanoparticles in azopolymers and it was attributed to the migration of the azopolymer around the undisplaced particle. Moreover, the large photo-induced collective mechanical forces can be affected by the π-π interaction, between the different components. MWCNTs, PAZO and DO3 can interact electrostatically through the different electronic clouds belonging to phenyl rings of DO3, PAZO or MWCNT. For higher surface/volume ratio, and therefore larger the area in contact between the MWCNT/DO3 agglomerate and PAZO, there is a higher probability of π-π stacking interaction between MWCNT/DO3 and PAZO.

In addition to the organization effect that we want to show in this work, a closer examination of the images reveals a secondary effect. All samples exhibit a sub pattern that consists of fringes of smaller period than the SRG. This effect is clearly visible in all the SEM images shown previously (Figs. 4–6). Fig. 7(a) shows a SEM of a cryogenic cut of a sample, from which we determine that the modulation depth of the secondary pattern is on the order of 15 nm. Supposing that the material is homogeneous, this small detail turns out to be more visible when the e-beam impinges normal on the sample substrate (Figs. 4–6), because of the scattering of electrons impinging at different angles on the sample surface. The darker areas are horizontal, while the shiny areas are at an angle different from zero with respect to the e-beam direction. Fig. 7(b) shows a MWCNT that lies down on the surface following the shape of this

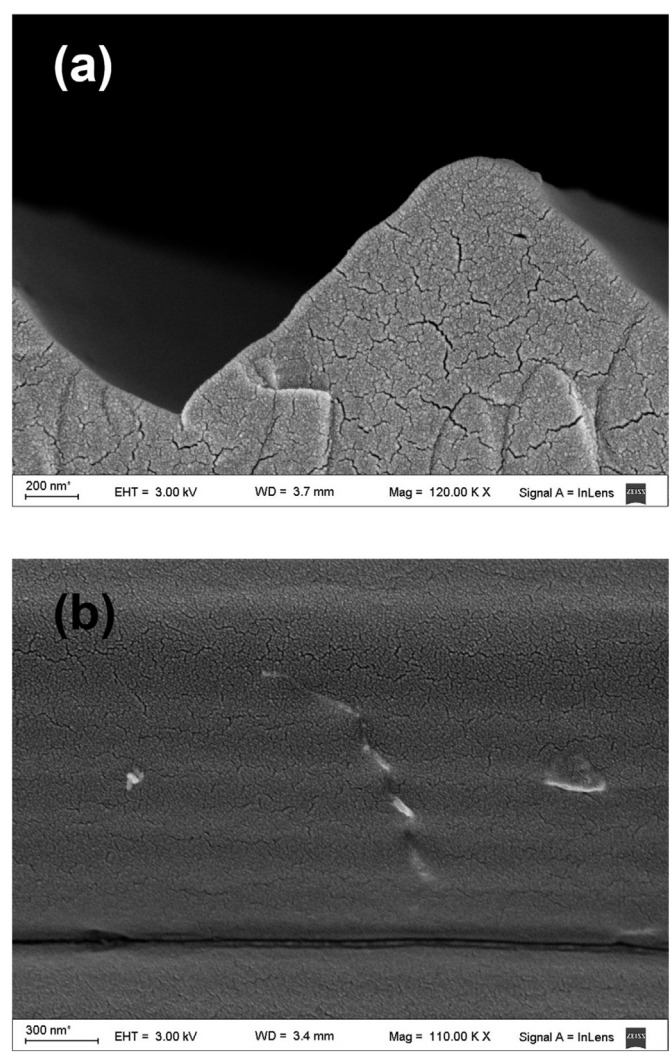

Fig. 7. (a) SEM image of a transversal section of a sample. (b) Isolated single MWCNT that lies on the subwavelength pattern that builds up on the crest of the SRG.

smaller period pattern. This fact suggests that once well dispersed MWCNTs are organized over the SRG in such a way that isolated MWCNT can be found over the surface of the polymer, the re-shaping of the polymer's surface through the mass transport could be potentially used to re-shape the MWCNT, as we will study in future work.

4. Conclusions

In this work we demonstrate the capability of using an azo-polymer film for large area organization of MWCNTs. Azopolymers were found to be an excellent platform to produce motions in the micro and nanoscale controlled remotely by light from the far field. Organization was achieved independently of the concentration of MWCNTs, but their location in different regions of the SRG was found to be dependent on the fabrication process. On the one hand, it was observed that depositing the MWCNTs after the recording of a SRG resulted in their localization in the troughs of the SRG. This was attributed to the mechanical forces acting during the spin coating of the MWCNTs solution. On the other hand, when depositing the MWCNTs before recording the SRG, the large photoisomerization forces dragged them to the crests of the SRG, that are located at the minima of the intensity distribution. Different concentrations of MWCNTs in the initial solution produces different structures of MWCNTs: isolated, small agglomerates or entangled nanotubes as a part of an expanded network. The latter produces a large deformation of the SRG due to the large dragging forces required to move an object with a high surface to volume ratio. Also, a larger surface to volume ratio maximizes the area in contact between the MWCNTs and the azopolymer. This increases the probability of interaction through π-π stacking between the MWCNTs and any of the azo-compounds (DO3 and PAZO) as well as the interaction between the two azo-compounds themselves. In the second case, DO3 can also mediate the interaction between MWCNTs and PAZO. When MWCNTs are dispersed in THF solution, one phenyl ring of a DO3 molecule is linked to a MWCNT through π-π stacking interaction, and the other remains free of interactions. The azobenzene molecule that is already present in the azopolymer has also one free phenyl ring, the other one is linked to the polymer backbone. The free phenyl rings (one in DO3 and other in PAZO) can also interact through π-π stacking, and then mediate the interaction between MWNTs and PAZO. Consequently, the surface to volume ratio matters when organizing nanostructures without SRG deformation. An interesting observation is that in the case of the SRG exhibiting a smaller modulation, a single MWCNT will locate on the surface following the shape of this modulation.

Acknowledgments

The authors would like to thank the financial support from the National Scientific and Technical Research Council – Argentina (CONICET, PIP 11220120100508CO), the University of Buenos Aires (UBACYT 20020130100495BA), ANPCyT (PICT 2012-1093, PICT-2014-3537, PICT 2014-2432) and the Basque Government (IT-776-13), and technical support from "Macrobehaviour-Mesostructure-Nanotechnology" SGIker unit from the University of the Basque Country.

Appendix A. Supplementary data

Supplementary data related to this article can be found at http://dx.doi.org/10.1016/j.optmat.2017.01.047.

References

[1] G.K. Knopf, Y. Otani, Optical Nano and Micro Actuator Technology, CRC Press, Boca Raton, Florida, 2013.
[2] J. Li Jianwei, Weihong Tan, A single DNA molecule nanomotor, Nano Lett. 2 (4) (2002) 315–318.
[3] B.L. Feringa, Molecular Switches, Wiley-VCH Verlag GmbH, Weinheim, FRG, 2001.
[4] Y. Wang, Q. Li, Light-driven chiral molecular switches or motors in liquid crystals, Adv. Mater. 24 (15) (2012) 1926–1945.
[5] T. Ikeda, M. Nakano, Y. Yu, O. Tsutsumi, A. Kanazawa, Anisotropic bending and unbending behavior of azobenzene liquid-crystalline gels by light exposure, Adv. Mater 15 (2003) 201–205.
[6] Y. Yu, M. Nakano, T. Ikeda, Directed bending of a polymer film by light, Nature 425 (2003) 145.
[7] H. Yu, T. Ikeda, Photocontrollable liquid-crystalline actuators, Adv. Mater 23 (19) (2011), 1521–4095.
[8] K.E. Snell, Photochromic Molecular Materials for the Controlled Organization of Nanoparticles, 2014. Electronic Thesis and Dissertation Repository. Paper 2474.
[9] Z. Sekkat, Optical tweezing by photomigration, Appl. Opt. 55 (2016) 259–268.
[10] J. Cambiasso, H. Garate, N. D'Accorso, S. Ledesma, S. Goyanes, Optical recording of stable holographic grating in a low Tg statistical copolymer covalently functionalized with an azo-dye, Opt. Mater 49 (2015) 141–146.
[11] F.-L. Ye, P.-Y. Gu, F. Zhou, H.-F. Liu, X.-P. Xu, H. Li, Q.-F. Xu, J.-M. Lu, Preparation of homopolymers from new azobenzene organic molecules with different terminal groups and study of their nonvolatile memory effects, Polymer 54 (13) (2013) 3324–3333.
[12] A. Natansohn, P. Rochon, J. Gosselin, S. Xie, Azo polymers for reversible optical storage 1 Poly[4'-[[2-(acryloyloxy)ethyl]ethylamino]-4-nitroazobenzene], Macromolec 25 (8) (1992) 2268–2273.
[13] A. Priimagi, A. Shevchenko, Azopolymer-based micro- and nanopatterning for photonic applications, J. Polym. Sci. Part B Polym. Phys. 52 (2014) 163–182.
[14] K.G. Yager, C.J. Barrett, Photomechanical surface patterning in azo-polymer materials, Macromolecules 39 (2006) 9320–9326.
[15] C. Rianna, A. Calabuig, M. Ventre, S. Cavalli, V. Pagliarulo, S. Grilli, P. Ferraro, P.A. Netti, Reversible holographic patterns on azopolymers for guiding cell adhesion and orientation, ACS Appl. Mater. Interfaces 7 (2015) 16984–16991.
[16] C. Rianna, L. Rossano, R.H. Kollarigowda, F. Formiggini, S. Cavalli, M. Ventre, P.A. Netti, Spatio-temporal control of dynamic topographic patterns on azo-polymers for cell culture applications, Adv. Funct. Mater (2016) 1–9.
[17] R.J. Moerland, J.E. Koskela, A. Kravchenko, M. Simberg, S. van der Vegte, M. Kaivola, A. Priimagi, R.H.A. Ras, Large-area arrays of three-dimensional plasmonicsubwavelength-sized structures from azopolymersurface-relief gratings, Mater. Horiz. 1 (2014) 74–80.
[18] L. Rocha, V. Dumarcher, C. Denis, P. Raimond, C. Fiorini, J.M. Nunzi, Laser emission in periodically modulated polymer films, J. Appl. Phys. 89 (2001) 3067–3069.
[19] L.M. Goldenberg, V. Lisinetskii, Y. Gritsai, J. Stumpe, S. Schrader, Single step optical fabrication of a DFB laser device in fluorescent azobenzene-containing materials, Adv. Mater 24 (2012) 3339–3343.
[20] K.E. Snell, N. Stephant, R.B. Pansu, J.F. Audibert, F. Lagugne-Labarthet, E. Ishow, Nanoparticle organization through photoinduced bulk mass transfer, Langmuir 30 (2014) 2926–2935.
[21] O. Watanabe, T. Ikawa, T. Kato, M. Tawata, H. Shimoyama, Area-selective photoimmobilization of a two-dimensional array of colloidal spheres on a photodeformed template formed in photoresponsive azopolymer film, Appl. Phys. Lett. 88 (2006) 86–89.
[22] Y. Li, Y. He, X. Tong, X. Wang, Photoinduced deformation of amphiphilic azo polymer colloidal spheres, J. Am. Chem. Soc. 127 (2005) 2402–2403.
[23] E. Ortyl, S. Zielinska, R. Barillé, Y. Almohamed, J.M. Nunzi, Instantaneous photoinduced patterning of an azopolymer colloidal nanosphere assembly, Opt. Mater. Express 6 (2016) 2925–2932.
[24] G.D. Costanzo, S. Ledesma, I. Mondragon, S. Goyanes, Stable solutions of multiwalled carbon nanotubes using an azobenzene dye, J. Phys. Chem. C 114 (2010) 14347–14352.
[25] J. Cambiasso, S. Goyanes, S. Ledesma, Holographic gratings recorded in poly(lactic acid)/azo-dye films, Opt. Mater 47 (2015) 72–77.